

Available online at [www.sciencedirect.com](http://www.sciencedirect.com)**SciVerse ScienceDirect**

Energy Procedia 14 (2012) 1464 – 1470

Energy

**Procedia**

2011 2nd International Conference on Advances in Energy Engineering (ICAEE 2011)

## Advanced State Feedback Control of Grid- Power Inverter

Marian Gaiceanu<sup>a,a\*</sup><sup>a</sup>*Dunarea de Jos University of Galati, Domneasca Street, No.47, 800008-Galati, Romania*

---

### Abstract

This paper shows the topology of grid-connected green power system and the performances of the front-end three-phase power inverter by applying an advanced state feedback control. The proposed topology benefits a common DC-AC inverter which injects the generated power into the grid. The control structure of the power inverter is of vector control type, in synchronous reference frame, and it uses the power balance concept. The solution presented in this paper adds supplementary benefits to the power system beside to the conventional state feedback control: the designed input filter assures zero steady state error and an adequate component is added for dynamic rejection of the load disturbance. The obtained experimental results are shown.

© 2011 Published by Elsevier Ltd. Selection and/or peer-review under responsibility of the organizing committee of 2nd International Conference on Advances in Energy Engineering (ICAEE). Open access under [CC BY-NC-ND license](http://creativecommons.org/licenses/by-nc-nd/3.0/).

*Keywords:* Renewable energy, power conditioning, grid-connected, advanced state feedback control

---

### 1. Introduction

The conventional energy sources (oil, natural gas, coal and nuclear) are finite and generate pollution. Alternatively, the renewable energy sources (any other source, which does not provide energy via fossil fuel combustion) are clean and abundantly available in nature [1], [2]. The basic principle of the alternative energy relates to issues of sustainability, renewability and pollution reduction [3]. In order to meet the continually increasing demand of the renewable power sources the power conditioning units are necessary. The main objective of the power conditioning system is to convert DC power from the renewable energy source (fuel cell/wind power) converter to AC power feeding the grid at maximum efficiency. The additional requirement for a power distribution system is to exchange the power between

---

\* Marian Gaiceanu. Tel.: +40-336-106-191; fax: +40-236-470-905.

E-mail address: [Marian.Gaiceanu@ieee.org](mailto:Marian.Gaiceanu@ieee.org).

the source and the load. Unlike the stand alone power conditioning, the grid connected one has the advantage of not using the batteries; thus, an increased efficiency is obtained. The proposed power conditioning system is suitable in applications in which the size and the weight have significant effect. The DC bus capacitor is the prime factor of degradation of power conditioning system reliability. By replacing the DC link electrolytic capacitor (which is bulky, heavy and suffers from the degradation of the electrolytic media, being a source of failures) the reliability of the system is improved, the size and the cost of the power unit decreasing. The consequence is that of increasing the lifetime of the power converter. The power quality function of the power conditioning system is assured by a proper control of the power system [4]. The grid converter is a full-bridge IGBT transistor-based converter and normally operates in inverter mode such that the energy is transferred from the renewable energy source to the utility grid and/or to the load. On the grid side, a di/dt-filter limits the rate of the current rise during the commutation of the current from a conducting freewheeling diode to a turning-on IGBT. Its main function is the limitation of the harmonic currents to a level that allows fulfilling IEEE 519-1992 even for very weak grids (down to a short circuit ratio of only 10) [5].

**2. The mathematical model of the dc-ac inverter**

The present paper is focused on the DC/AC stage because this acts as grid inverter and determines the overall performances of the power system. In order to design the DC/AC control it is necessary to write the differential equations of the system.

The current model in the *q-d* reference frame is represented by the following first-order differential equations:

$$\begin{aligned} \frac{dI_D}{dt} + \omega \cdot I_Q &= -\frac{1}{L} \cdot V_D + \frac{1}{L} \cdot E_D \\ \frac{dI_Q}{dt} - \omega \cdot I_D &= -\frac{1}{L} \cdot V_Q + \frac{1}{L} \cdot E_Q \end{aligned} \tag{1}$$

where  $E_Q$  and  $E_D$  are the *q-d* mains voltage components,  $I_Q$  and  $I_D$  are the *q-d* line current components,  $L$  is the line inductance,  $V_D$  and  $V_Q$  are the voltages of the input DC-AC power inverter, that differ from the  $E_Q$  and  $E_D$  voltages because of the boost inductor, as shown also in Fig. 1.

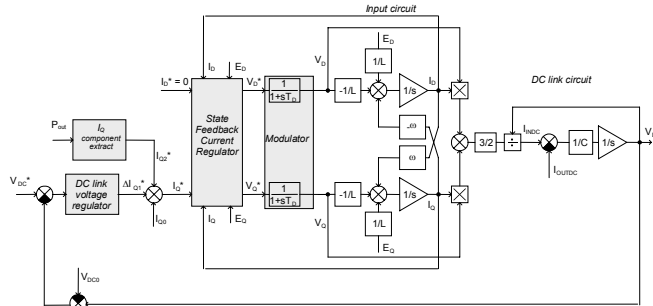


Fig. 1 The control block diagram of the source side converter.

The decoupled inverter vectorial equation is:

$$\vec{E} = L \cdot \frac{d\vec{I}}{dt} + \vec{V} \tag{2}$$

It is necessary to find the relation between the  $I_Q - I_D$  currents and the DC link voltage,  $V_{dc}$ . The dc link input power of the DC-AC inverter has the form:

$$P_{inDC} = V_{dc} I_{inDC} \tag{3}$$

where  $I_{inDC}$  is the DC link input current (Fig.1).

The AC power of the DC-AC inverter, in  $q$ - $d$  reference frame, is as follows:

$$P_{AC} = \frac{3}{2} \cdot (V_D \cdot I_D + V_Q \cdot I_Q) \quad (4)$$

Moreover, the equation between the capacitor current and the voltage, with reference to the variable definitions depicted in Fig. 1, is

$$C \cdot \frac{dV_{dc}}{dt} = I_{inDC} - I_{outDC} \quad (5)$$

Therefore, the DC output current is obtained from the power balance by using eqs (3,4),

$$I_{outDC} = \frac{3}{2} \cdot \frac{V_D \cdot I_D + V_Q \cdot I_Q}{V_{dc}} \quad (6)$$

By aligning the  $q$  axis with the main voltage vector  $\vec{E}$  through PLL circuit, the  $E_d$  supply voltage  $d$ -component becomes zero:

$$\vec{E} = E_Q + j \cdot E_D, \text{ with } E_D = 0 \text{ and } E_Q = E, \quad (7)$$

where  $E$  is the maximum value of the grid phase voltage.

The modulation system has been modelled by using a first order transfer function with a pole at  $1/T_D$ . The PWM modulator introduces a IGBT switch delay, namely dead time. This delay  $T_D$  is approximately equal to half the of  $T_s$ , the switching frequency

### 3. The current control of the dc-ac power inverter

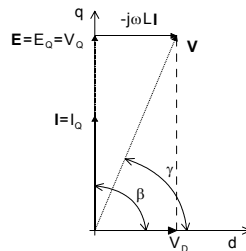


Fig. 2 Input voltage and current supply vectors in the synchronously reference frame at unitary power factor operation

The goal of the current loop is to impose the sinusoidal current absorption from the supply with unitary power factor. The current control system has been implemented in synchronously,  $q$ - $d$  reference frame. By using synchronous rotating-frame current regulators in the source (ac-dc) converter side, the active and reactive power can be controlled independently.

In order to impose a unitary power factor ( $\cos(\theta) = 1$ , where  $\theta$  is the angle between the current and the voltage supply), it is sufficient to set up the direct current reference,  $I_D^*$ , to zero. In such a case, the current vector lies on the  $q$  axis and consequently, it is in phase with the  $\vec{V}$  vector, like in Fig. 2. Clearly, if a  $\cos(\theta) < 1$  is desired (in order to absorb a reactive power from the supply), it will be sufficient to act on the  $I_D^*$  value.

**3.1. Design of the current state feedback controller in synchronous reference frame.**

In order to design the state feedback controller, a standard state space representation of the DC/AC system has been deduced from Eq. (1):

$$\begin{cases} \dot{\mathbf{x}} = \mathbf{A} \cdot \mathbf{x} + \mathbf{B} \cdot \mathbf{u} + \mathbf{F} \cdot \mathbf{e} \\ \mathbf{y} = \mathbf{C} \cdot \mathbf{x} \end{cases} \Rightarrow \begin{cases} \begin{bmatrix} \dot{I}_D \\ \dot{I}_Q \end{bmatrix} = \begin{bmatrix} 0 & -\omega \\ \omega & 0 \end{bmatrix} \cdot \begin{bmatrix} I_D \\ I_Q \end{bmatrix} + \begin{bmatrix} -\frac{1}{L} & 0 \\ 0 & -\frac{1}{L} \end{bmatrix} \cdot \begin{bmatrix} V_D^* \\ V_Q^* \end{bmatrix} + \begin{bmatrix} \frac{1}{L} & 0 \\ 0 & \frac{1}{L} \end{bmatrix} \cdot \begin{bmatrix} E_D \\ E_Q \end{bmatrix} \\ y = \begin{bmatrix} 1 & 0 \\ 0 & 1 \end{bmatrix} \cdot \begin{bmatrix} I_D \\ I_Q \end{bmatrix} \end{cases} \quad (8)$$

The control action consists mainly of three components: the state feedback, the pre-filter placed on the reference channel, and the direct compensation of the disturbances [6]:

$$\mathbf{u} = \mathbf{G}\mathbf{x} + \mathbf{K}\mathbf{y}^* + \mathbf{R}\mathbf{e} \quad (9)$$

where  $\mathbf{G} = \begin{bmatrix} G_{11} & G_{12} \\ G_{21} & G_{22} \end{bmatrix}$ ,  $\mathbf{K} = \begin{bmatrix} K_{11} & K_{12} \\ K_{21} & K_{22} \end{bmatrix}$ ,  $\mathbf{R} = \begin{bmatrix} R_{11} & R_{12} \\ R_{21} & R_{22} \end{bmatrix}$  are the adequate matrices.

The structure of the state-feedback control system and the system control are depicted in Figure 2.

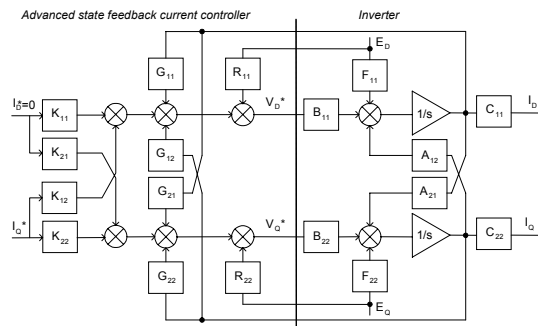


Fig. 3 The advanced state-feedback current control

Since  $R_{12}=R_{21}=0$  (due to the structure of the system under control), these gains have not been reported in Figure 3.

By substituting the control expression (9) in the system under control (8), the controlled system is obtained in standard form:

$$\begin{cases} \dot{\mathbf{x}} = (\mathbf{A} + \mathbf{B} \cdot \mathbf{G}) \cdot \mathbf{x} + \mathbf{B} \cdot \mathbf{K} \cdot \mathbf{y}^* + \mathbf{B} \cdot \mathbf{R} \cdot \mathbf{e} + \mathbf{F} \cdot \mathbf{e} \\ \mathbf{y} = \mathbf{C} \cdot \mathbf{x} \end{cases} \quad (10)$$

In order to cancel the perturbation effect,  $e$ , the  $\mathbf{R}$  gain must be chosen such that:

$$\mathbf{R} = -\mathbf{B}^{-1} \cdot \mathbf{F} \quad (11)$$

By imposing the zero steady state error, the pre-filter gain value,  $\mathbf{K}$ , on the input reference is provided:

$$\mathbf{K} = -\mathbf{B}^{-1} \cdot (\mathbf{A} + \mathbf{B} \cdot \mathbf{G}) \cdot \mathbf{C}^{-1} \quad (12)$$

By using the pole placement method, the final value of the **G** gain is determined. The closed loop eigenvalues are assigned by imposing an adequate time response  $T_R$  and a damping factor  $d$ , which yields:

$$\lambda_{1,2} = -d \cdot \omega_0 \pm \omega_0 \cdot \sqrt{1-d^2}i \tag{13}$$

where

$$\omega_0 = \frac{1}{d \cdot T_R} \cdot \left( 3 - \frac{1}{2} \ln(1-d^2) \right) \tag{14}$$

The feedforward current component was added to the reference (Fig.1). Its value is provided from the power balance equation, i.e. the power converter must meet the load power requirements. Therefore,

$$I_{q2}^* = \frac{2}{3E} \cdot P_{out} \tag{15}$$

Through the feedforward component, since  $E$  is constant, the active power flow is controlled indirectly by the reference current. The output power,  $P_{out}$  (19), is estimated from the inverter terminals.

A unity power factor is necessary in AC drive. This implies a proper orientation of the reference frame and a zero  $d$ -axis current reference value:

$$I_d^* = 0 \tag{16}$$

By linearizing (5) through the small perturbation method around the equilibrium point, the parameters of the dc-voltage controller are derived. The method of *symmetrical optimum* in Kessler variant [4]

(the amplitude and the phase plot are symmetrical given the crossover frequency), was used in order to synthesize the voltage controller parameters by using open-loop transfer function. The main task of the voltage controller is to maintain the dc link voltage to a certain value. Another task is to control the voltage converter power flow.

#### 4. Experimental results

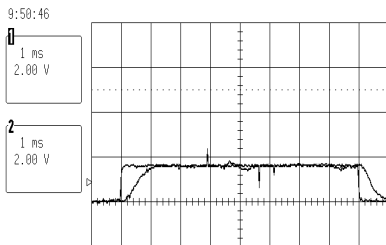


Fig. 4 The input and the output signals of the  $d$  axis current loop: Ch.1: the  $d$  axis current reference 50A/div. Ch.2: the actual  $d$  axis current.

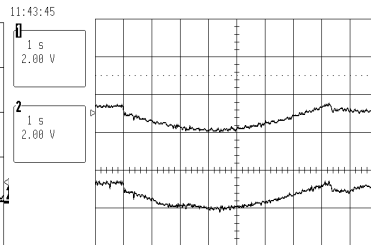


Fig. 5 The input and the output signals of the  $q$  axis current loop: Top trace (Ch.1): the  $q$  axis current reference,  $I_q^*$  50A/div. Bottom trace (Ch.2): the actual  $q$  axis current,  $I_q$ .

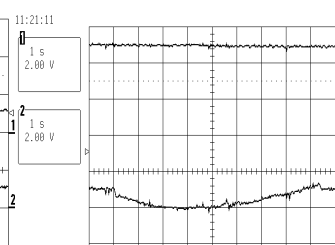


Fig. 6 Ch1 – The dc link voltage,  $V_{dc}$  190V/div, Ch2- the actual load current of the supply converter,  $I_q$  50 A/div.

The power stage of the 37-kW prototype unit is based on two 1200V IGBTs three-phase voltage power modules followed by SKHI drive types from Semikron. The power semiconductor switches are operated with  $T_s=125\mu s$  switching time. The power flow of the grid side inverter is controlled in order to keep the DC-link voltage constant. The control structure of the grid-power inverter is of vector control type, in synchronous reference frame, and it uses the power balance concept.

The capacitor bank has two parallel connected 500 $\mu F$  film capacitors with 900V dc rating voltage. The line inductance of the grid-power inverter has  $L=0,5$  mH value. By choosing the response time  $T_r = 0.6e-3$  and the damping coefficient  $d = 0.707$ , the following desired poles of the closed loop system are

obtained  $\mathbf{P} = \begin{bmatrix} 11 & 12 \end{bmatrix} = 1.0e+003 * \begin{bmatrix} -5.5774 + 5.5791i & -5.5774 - 5.5791i \end{bmatrix}$ . Knowing the output inductance, based on the above mentioned design expressions, the state-feedback controller has been designed by using the Matlab software. Thus, the following matrices:  $\mathbf{G} = \begin{bmatrix} 2.7887 & 2.6324 \\ -2.6324 & 2.7887 \end{bmatrix}$ ;  $\mathbf{K} = \begin{bmatrix} -2.7887 & -2.7895 \\ 2.7895 & -2.7887 \end{bmatrix}$  and  $\mathbf{R} = \begin{bmatrix} 1 & 0 \\ 0 & 1 \end{bmatrix}$  are obtained.

The stationary and transient performances are presented in (Figs.4-8) in order to show the effectiveness of the proposed control strategy for the grid inverter. Less than 5% current THD factor (under rated power level) and a unity power factor operation have been obtained.

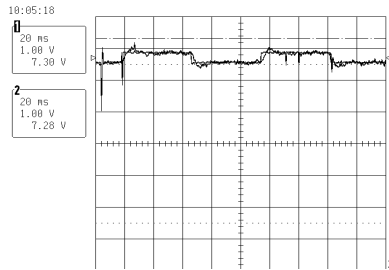


Fig. 7 DC-link voltage controller: Ch.1: the dc link voltage reference,  $V_{DC}^*$ . Ch.2: the actual dc link voltage,  $V_{DC}$ , 230V/div.

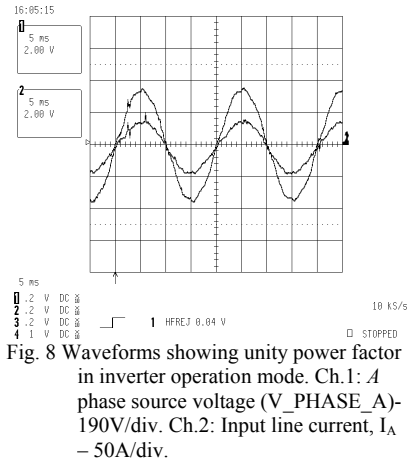


Fig. 8 Waveforms showing unity power factor in inverter operation mode. Ch.1: A phase source voltage ( $V_{PHASE\_A}$ ) - 190V/div. Ch.2: Input line current,  $I_A$  - 50A/div.

The performances of the grid - power inverter current controllers are presented by the Fig. 6, for  $q$ -axis (load) current component. A test current generator was used in order to obtain the  $d$ -axis current reference waveforms (Fig.4). The reference of the source load current (Fig.5) has ripples in transients to regulate the dc-link voltage and the power matching control. The actual load current,  $I_q$ , accurately follows its reference  $I_q^*$  (Fig.5). In the Fig. 7 the performances of the dc-link voltage controller are shown. The ripple in the dc-link voltage appears due to the delay of the digital control.

Additionally, the Figs. 4-7 show the performances of the grid current controller and of the dc-link voltage controller. Power matching control is proved by no DC voltage variation to the change of the rated load in normal (Fig.6) operation mode. The trace of the  $A$  phase of the grid current is in phase with  $A$  phase of the grid voltage, which clearly demonstrates the unity power factor operation (Fig. 8).

## 5. Conclusion

This topology assures a constant DC link voltage, the integration of the renewable energy into the grid, the power quality issues, the active and reactive decoupled power control, and the grid synchronization. This paper presents the performances of the grid connected power inverter, which works properly based on advanced state feedback current controllers. The state feedback current controllers assure fast disturbance rejection resulting in low dc-link ripple voltage, zero steady state and a stable power system. By maintaining a constant dc link voltage, the dc link current follows the load levels requirements. The resulted grid connected inverter has the following advantages: reduction of the lower order harmonics in the ac line current, constant dc-link voltage, nearly unity efficiency, zero displacement between voltage and current fundamental component, power reversibility capabilities as well as a good power matching control, disturbance compensation capability, fast control response and high quality balanced three-phase output voltages, small (up to 5%) ripple in the dc-link voltage in any operating conditions.

## References

- [1] Enslin J.H.R.. *Opportunities in Hybrid Energy Networks using Power Electronic Interfaces*, Future Power Systems, 2005 International Conference on 16-18 Nov., 2005, p.1 – 7.
- [2] Joos G., Ooi B.T, McGillis D., Galiana F.D., Marceau R. (2000). The potential of distributed generation to provide ancillary services, *IEEE Power Engineering Society Summer Meeting*, 16-20 July, Vol. 3, pp. 1762 – 1767.
- [3] Agbossuo K, Chahine R, Hamelin J, Laurencelle F, Hamelin J. Renewable energy systems based on hydrogen for remote applications, *Journal of Power Sources*, 2001, **96**:168–172.
- [4] Gaiceanu M. AC-AC Converter System for AC Drives, British Library, London, Publisher: Institution of Electrical Engineers, Printed in Great Britain by WRIGHTSONS, ISSN 0537-9989, *IEE Conference Publication Journal* 2004; Vol. 2, 498: 724-729.
- [5] IEEE Std 519-1992. IEEE Recommended Practices and Requirements for Harmonic Control in Electrical Power Systems, *IEEE Industry Applications Society/Power Engineering Society*, Published by the Institute of Electrical and Electronics Engineers, Inc., 345 East 47th Street, New York, NY 10017 USA, April 12, 1993.
- [6] Uhrin R, Profumo F., State Feedback Current Regulator for Quasi Direct AC/AC Converter, EDPE, Conference record, 1996.